AD-A134 456 COMPUTATION OF SURFACE SHIP WAVE PROFILES WITH THIN SHIP THEORY(U) DAVID W TAYLOR NAVAL SHIP RESEARCH AND DEVELOPMENT CENTER BETHESDA MD Y S HONG SEP 83 1/1

UNCLASSIFIED F/G 12/1 NL

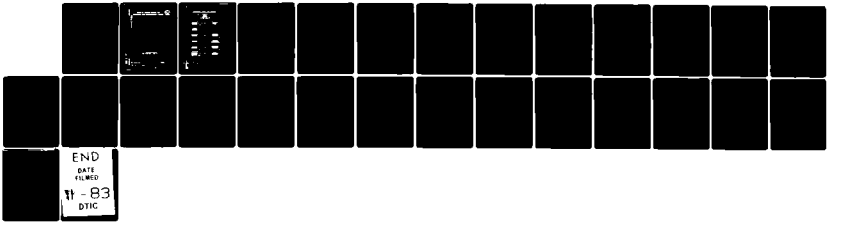

END
DATE FILMED
11-83
DTIC

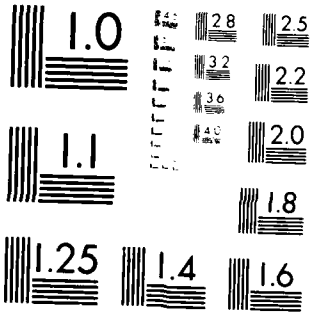

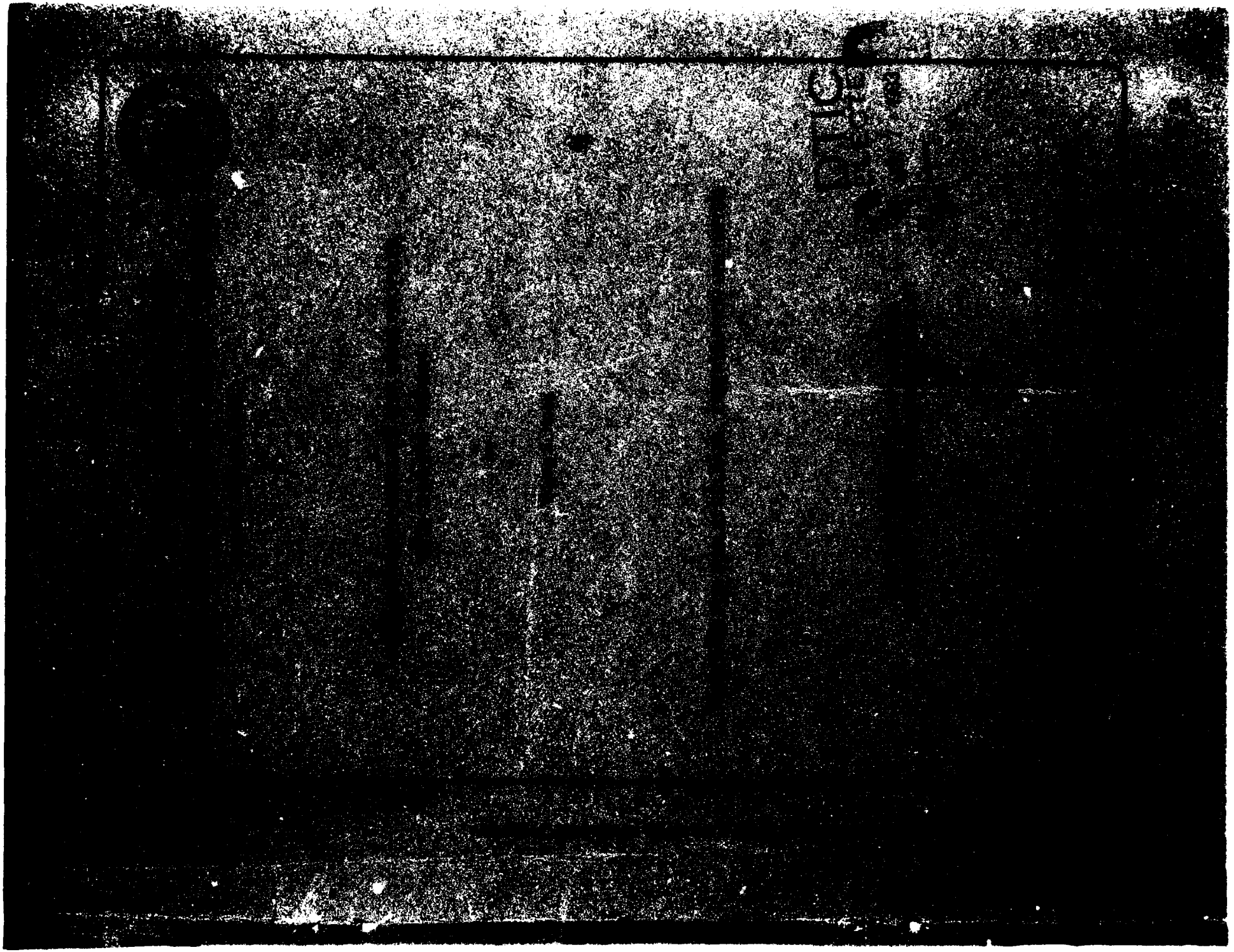

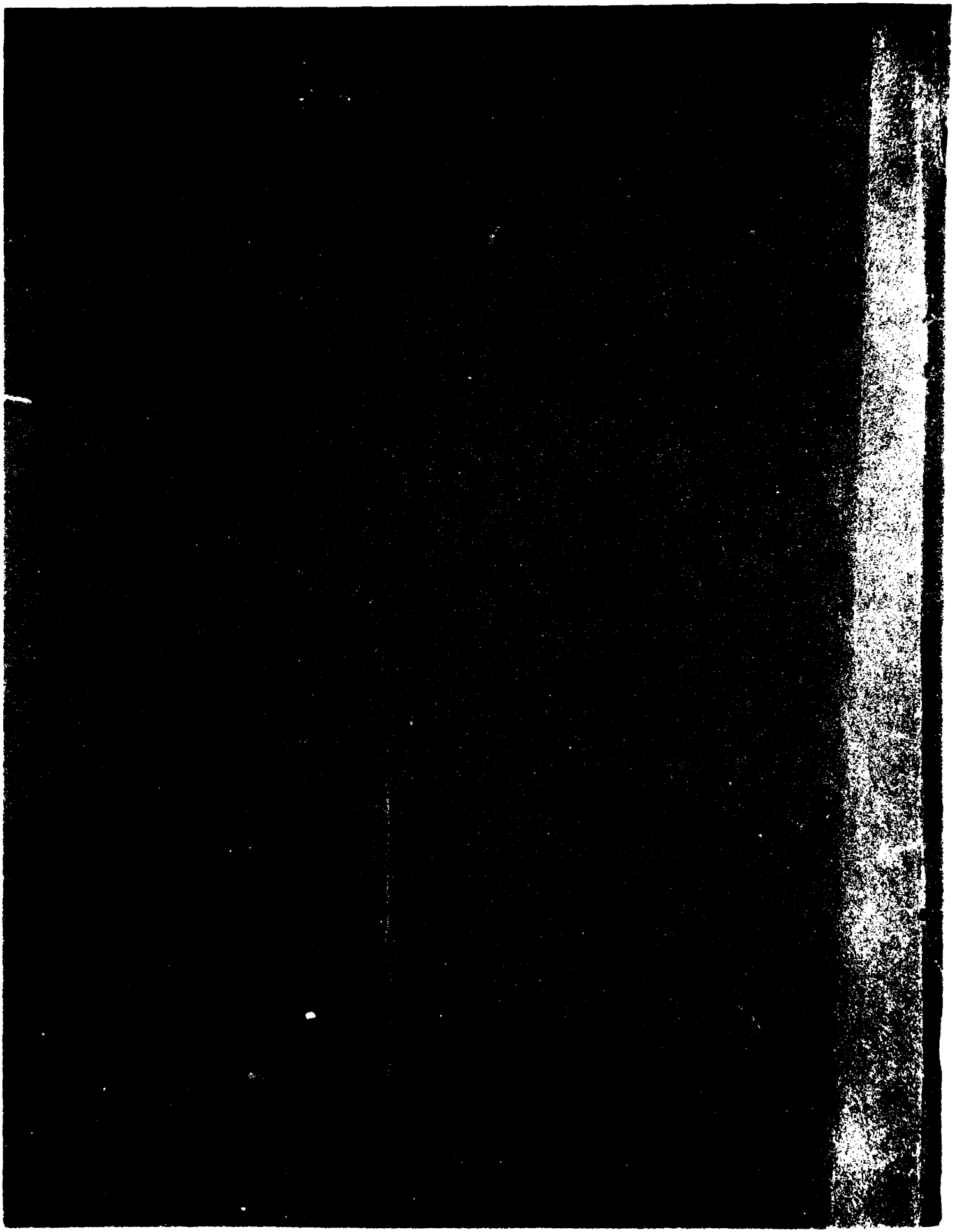

UNCLASSIFIED

SECURITY CLASSIFICATION OF THIS PAGE (When Data Entered)

REPORT DOCUMENTATION PAGE	READ INSTRUCTIONS BEFORE COMPLETING FORM
1 REPORT NUMBER: DTNSRDC-83/062 — 2 GOVT ACCESSION NO: A134456	3 RECIPIENT'S CATALOG NUMBER
4 TITLE (and Subtitle): COMPUTATION OF SURFACE SHIP WAVE PROFILES WITH THIN SHIP THEORY	5 TYPE OF REPORT & PERIOD COVERED: Final
	6 PERFORMING ORG. REPORT NUMBER
7 AUTHOR(s): Young S. Hong	8 CONTRACT OR GRANT NUMBER(s)
9 PERFORMING ORGANIZATION NAME AND ADDRESS: David W. Taylor Naval Ship Research and Development Center, Bethesda, Maryland 20084	10 PROGRAM ELEMENT, PROJECT, TASK AREA & WORK UNIT NUMBERS: (See reverse side)
11 CONTROLLING OFFICE NAME AND ADDRESS	12 REPORT DATE: September 1983
	13 NUMBER OF PAGES: 25
14 MONITORING AGENCY NAME & ADDRESS(if different from Controlling Office)	15 SECURITY CLASS. (of this report): UNCLASSIFIED
	15a DECLASSIFICATION DOWNGRADING SCHEDULE

16 DISTRIBUTION STATEMENT (of this Report)

APPROVED FOR PUBLIC RELEASE: DISTRIBUTION UNLIMITED

17 DISTRIBUTION STATEMENT (of the abstract entered in Block 20, if different from Report)

18 SUPPLEMENTARY NOTES

19 KEY WORDS (Continue on reverse side if necessary and identify by block number)

Surface Ship Wave Profile

20 ABSTRACT (Continue on reverse side if necessary and identify by block number)

A computational method of free-surface wave-height prediction for a ship in steady motion has been developed through application of Michell's thin ship theory. Numerical computation for two different hulls has been presented. The results for the Wigley hull agree well with the experiment. However, the agreement between the numerical results and the experiment for

(Continued on reverse side)

DD FORM 1 JAN 73 1473 EDITION OF 1 NOV 65 IS OBSOLETE
S/N 0102-LF-014-6601

UNCLASSIFIED

SECURITY CLASSIFICATION OF THIS PAGE (When Data Entered)

(Block 10)

Task Area SR0230101
Program Element 61153N
Work Unit 1542-700

(Block 20 continued)

the SL7 container ship is not satisfactory. Further study in the analytical method is necessary to improve the numerical results for a ship with a bulbous bow.

A-1

TABLE OF CONTENTS

LIST OF FIGURES

LIST OF TABLES

NOTATION

A_{ij}, B_{ij}, C_{ij}, D_{ij}, E_j, F_j	Coefficients for piecewise hull function
a	$k_o y'$
B	Breadth
B_1	Slope of a linear function
B_2	Constant of a linear function
b	$k_o(x-x')$
F_n	Froude number
f	Hull Function
G	Green function
g	Gravitational acceleration
H	Draft
H(x)	Heaviside function
I, J, Q	Integral notation
k_o	g/U^2
L	Length
ℓ, t, u, x, x', y', θ	Variables
n	Positive integer number
t_1	$(2n+1/2)\pi$ or $2n\pi$
t_2	$(2n+2+1/2)\pi$ or $(2n+2)\pi$
U	Speed
η	Free-surface wave height
ρ	Water density
ϕ	Velocity potential

ABSTRACT

A computational method of free-surface wave height prediction for a ship in steady motion has been developed through application of Michell's thin ship theory. Numerical computation for two different hulls has been presented. The results for the Wigley hull agree well with the experiment. However, the agreement between the numerical results and the experiment for the SL7 container ship is not satisfactory. Further study in analytical method is necessary to improve the numerical results for a ship with a bulbous bow.

ADMINISTRATIVE INFORMATION

This work was performed under the General Hydromechanics Research Program and was authorized by the Naval Sea Systems Command (NAVSEA), Hull Research and Technology Office. Funding was provided under Program Element 61153N, Task Area SR 0230101, and Work Unit 1542-700.

INTRODUCTION

The analytical method for computing the free-surface wave height of a ship is one of the most important tasks in naval hydrodynamics. The steady ship wave profile is usually linearly superimposed on other free-surface wave profiles. In the computation of the relative bow motion of a naval ship in waves, it is necessary to know the wave height due to the steady forward motion before computing the transfer functions. The analytical study of deck wetness also requires the knowledge of the wave profiles in steady motion.

The present computational method has been developed through an application of Michell's thin ship theory. This theory is first-order and linearized. Even though there is some limitation in the application of thin ship theory to ships with large block coefficients and with blunt bows, the results of this theory are reliable for various hull forms as concluded in Reference 1.*

Two hull forms have been chosen for the numerical computations in this presentation: a Wigley hull and an SL7 container ship. The numerical results for the Wigley hull, which is a mathematical hull form, show satisfactory agreement with the experiment. However, the numerical results for the SL7 are not satisfactory. There are some discrepancies near the bow region for even small Froude numbers.

---

*A complete listing of references is given on page 17.

EQUATIONS OF FREE-SURFACE WAVE HEIGHT

The coordinate system o,x,y,z is fixed in the ship with o,x,y containing the longitudinal centerplane, o,y,z the midship section, and o,x,z the undisturbed water surface if the ship is at rest. The vector o,x points toward the stern, and the ship is moving with speed U toward the negative x-axis. With assumptions that the fluid is inviscid and the flow is irrotational, the governing equation and boundary conditions are:[2]

(i) in the fluid domain

$$\phi_{xx} + \phi_{yy} + \phi_{zz} = 0 \tag{1}$$

(ii) Bernoulli's equation on the free surface

$$\frac{\rho}{2} [(\phi_x - U)^2 + \phi_y^2 + \phi_z^2] + \rho g y + p = \text{const.} \tag{2}$$

(iii) on the body surface, $z = f(x,y)$

$$f_x (\phi_x - U) + f_y \phi_y - \phi_z = 0 \tag{3}$$

(iv) on the free surface, $y = \eta(x,z)$

$$\eta_x (\phi_x - U) - \phi_y + \eta_z \phi_z = 0 \tag{4}$$

Equations (2), (3), and (4) are exact boundary conditions. In order to derive the solution of the thin ship theory, it is necessary to linearize these equations with the assumptions that the derivatives of ϕ, f, and η are small and, hence, second degree terms are negligible. The linearized conditions become

(ii) free surface condition

$$\phi_{xx} + k_o \phi_y = 0 \tag{5}$$

(iii) body boundary condition

$$\phi_z = U f_x \tag{6}$$

(iv) the free-surface wave height

$$\eta = \frac{U}{g} \phi_x (x,0,0) \tag{7}$$

The solution of Equation (1) with the boundary conditions, Equations (5) and (6), is given by

$$\phi(x,y,z) = \frac{U}{2\pi} \iint G(x,y,z;x',y',0) f_{x'}(x',y') dx'dy' \tag{8}$$

where G is the Green function as given in Reference 2 as

$$G(x,y,z;x',y',z') = -\frac{1}{r} + \frac{1}{r_1} + \frac{4k_o}{\pi} \int_0^{\frac{\pi}{2}} \sec^2\theta \, d\theta \int_0^{\infty} dk \exp[k(y+y')]$$

$$\times \frac{\cos[k(x-x')\cos\theta] \cos[k(z-z')\sin\theta]}{k - k_o\sec^2\theta} + 4\pi k_o \int_0^{\frac{\pi}{2}} d\theta \sec^2\theta$$

$$\times \exp[k_o(y+y')\sec^2\theta] \sin[k_o(x-x')\sec\theta]$$

$$\cos[k_o(z-z')\sin\theta \cdot \sec^2\theta) \tag{9}$$

where $k_o = g/U^2$

$r = [(x-x')^2+(y-y')^2+(z-z')^2]^{1/2}$

$r_1 = [(x-x')^2+(y+y')^2+(z-z')^2]^{1/2}$

Here, (x,y,z) is the point where the potential is sought and (x',y',z') is a source point. With substitution of Equation (8) into Equation (7) and integrating by parts, the free-surface wave height becomes

$$\eta = \frac{U^2}{2\pi g} \left\{ \iint G(x,0,0;x',y',0) f_{x'x'} dx'dy' - \int G f_{x'} dy' \Big|_{x'=-\frac{L}{2}}^{\frac{L}{2}} \right\} \qquad (10)$$

The fact that $G_{x'} = - G_x$ has been applied in the derivation of Equation (10).

NUMERICAL COMPUTATION

In order to simplify the numerical computation, Equation (9) is expressed in different form[3]

$$G(x,0,0;x',y',0) = I + J$$

$$= \frac{4k_o}{\pi} \int_0^{\frac{\pi}{2}} \sec^2\theta \, d\theta \int_0^{\infty} \frac{(\ell + k_o y' \sec^2\theta) \, e^{-\ell} \, d\ell}{(\ell + k_o y' \sec^2\theta)^2 + [k_o(x-x')\sec^2\theta]^2}$$

$$- 8H(x-x') \, k_o \int_0^{\frac{\pi}{2}} \sec^2\theta \, e^{k_o y' \sec^2\theta} \sin [k_o(x-x')\sec\theta] \, d\theta \qquad (11)$$

where $H(x)$ is the Heaviside function, defined as 1 for $x > 0$, 0 for $x < 0$, and 1/2 for $x = 0$. By substitution of Equation (11) into Equation (10), the free-surface wave height is expressed as

$$\eta = \frac{U^2}{2\pi g} \left\{ \iint (I+J) f_{x'} dx' dy' - \int (I+J) f_{x'} dy' \Big|_{x'=-\frac{L}{2}}^{\frac{L}{2}} \right\} \tag{12}$$

The first term of Equation (11) can be rewritten as given in Reference 4

$$I = \int_0^{\frac{\pi}{2}} d\theta \int_0^{\infty} \frac{(\ell\cos^2\theta + k_o y') \, e^{-\ell} \, d\ell}{(\ell\cos^2\theta + k_o y')^2 + [k_o(x-x')\cos\theta]^2}$$

$$= \int_0^{\frac{\pi}{2}} Q(a,b,\theta) \, d\theta \tag{13}$$

where

$$Q(a,b,\theta) = \int_0^{\infty} \frac{(\ell\cos^2\theta + a) \, e^{-\ell} \, d\ell}{(\ell\cos^2\theta + a)^2 + b^2 \cos^2\theta} \tag{14}$$

with $a = k_o y'$ and $b = k_o(x-x')$. The general behavior of the integrand of $Q(a,b,\theta)$ is explained in detail in Reference 4. The method of numerical evaluation of $Q(a,b,\theta)$ in this report is different from that of Reference 4. In this representation the integrand is differentiated with respect to ℓ and set to zero in order to find extreme values with $\ell\cos^2\theta + a = v$, the maximum or minimum values of the integrand occur in the following solution

$$v^3 + \cos^2\theta \cdot v^2 + b^2\cos^2\theta \cdot v - b^2\cos^4\theta = 0 \tag{15}$$

There are three complex solutions of Equation (15) which may be designated as v_1, v_2, and v_3 where the maximum or minimum values occur in the integrand of 0.

$$\ell_1 = \frac{v_1 - a}{\cos^2\theta}, \quad \ell_2 = \frac{v_2 - a}{\cos^2\theta}, \quad \ell_3 = \frac{v_3 - a}{\cos^2\theta} \tag{16}$$

Only the real solutions are used in the numerical evaluation, and, in most cases, there will be one or two real solutions. If there are two real solutions, these two solutions are separated from the point $\ell_o = -a/\cos^2\theta$. At this point the integrand of Q becomes zero. This case is represented graphically in Figure 1.

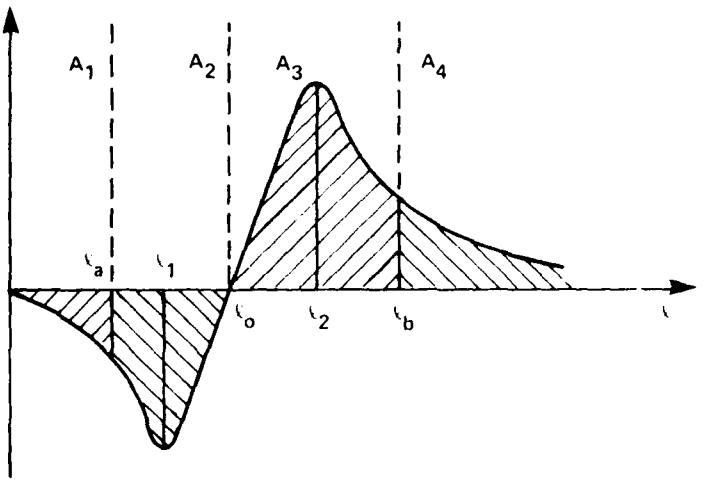

Figure 1 - Integral Regions of Q

For example, if there are two solutions, the integral region is subdivided into four subregions: $A_1(0 \leq \ell < \ell_a)$, $A_2(\ell_a \leq \ell < \ell_o)$, $A_3(\ell_o \leq \ell < \ell_b)$, and $A_4(\ell_b \leq \ell < \infty)$. Here, ℓ_a and ℓ_b are determined as follows

$$\ell_a = \ell_1 - K(\ell_o - \ell_1) \tag{17}$$

and

$$\ell_b = \ell_2 + K(\ell_2 - \ell_o) \tag{18}$$

where K is a constant which depends upon a, b, and θ. The specific value of the constant K which is employed in any particular computation falls between 1 and 10

and is found by examining the numerical stability of the algorithm. Each hull form and operating condition may require the setting of different integration limits. The process of selection of K is straightforward but is not automatic, and requires the attention of the investigator. When a and b are small, the integrand of Q increases slowly between 0 and ℓ_1, and then decreases rapidly between ℓ_1 and ℓ_o. Between ℓ_o and ℓ_2, the integrand increases rapidly and decreases slowly when ℓ is larger than ℓ_2. Therefore, the discretized distances for numerical integration are different in those subregions. In subregion A_2 and A_3, for example, the integration step is smaller than that of A_1 and A_4. This approach is employed in order to reduce computational time.

In each region, the integrand of Q is computed numerically. As a special case, when $\vartheta = \pi/2$, Equation (14) becomes

$$Q\left(a,b,\frac{\pi}{2}\right) = \frac{1}{a} \tag{19}$$

In order to show the behavior of the Q-function, the integrated values at each region are given in Table 1 for a = -0.12 and b = 1.0. The first column indicates the ϑ-variable and the following three column pairs show the integrated values of Q at three different divisions: A_1, A_2, and A_3. The last column is the total Q-values at each given ϑ. The integral of the last column with respect to ϑ becomes the result of I-integral The integrated values of Q are small positives when ϑ is about 70 deg and less in this case. For higher ϑ, Q becomes large and negative. The I-integral is always negative.

In the computational procedure, the I-integral is substituted into Equation (12), and the first and third terms are computed numerically.

The second term of Equation (11) can be rewritten with change of variable, $\sec\vartheta = t$ as follows

$$J = -8k_o H(x-x') \int_1^\infty \frac{t\, e^{k_o y' t^2}}{\sqrt{t^2-1}} \sin\left[k_o(x-x')t\right] dt \tag{20}$$

TABLE 1 - NUMERICAL EXAMPLE OF $Q(-0.12, 1.0, \theta)$

θ(deg)	A_1	Q_1	A_2	Q_2	A_3	Q_3	$Q=Q_1+Q_2+Q_3$
0.0	0- 0.1200	-0.00687	0.1200- 1.2074	0.18422	1.2074-14.0	0.12057	0.29792
15.0	0- 0.1286	-0.00786	0.1286- 1.2373	0.18917	1.2373-14.0	0.12248	0.30378
30.0	0- 0.1600	-0.01203	0.1600- 1.3362	0.20389	1.3362-14.0	0.12788	0.31975
45.0	0- 0.2400	-0.02624	0.2400- 1.5413	0.22528	1.5413-14.0	0.13459	0.33363
60.0	0- 0.4800	-0.09587	0.4800- 1.9843	0.22815	1.9843-14.0	0.12987	0.26215
70.0	0- 1.0258	-0.35972	1.0258- 2.7171	0.16130	2.7171-14.0	0.09161	-0.10680
80.0	0- 3.9796	-2.25960	3.9796- 5.8742	0.01016	5.8742-14.0	0.00621	-2.24320
83.0	0- 8.0796	-4.01370	8.0796-10.024	0.00018	10.024 -14.0	0.00011	-4.01340
86.0	0-14.000	-6.35960					-6.35960
87.0	0-14.000	-7.12090					-7.12090
88.0	0-14.000	-7.75970					-7.75970
88.4	0-14.000	-7.96170					-7.96170
88.8	0-14.000	-8.12510					-8.12510
90.0		-8.33333					-8.33333
							I = -0.77498

If $f_{x'x'}$ is expressed in Equation (12) as

$$f_{x'x'} = A_{ij} + B_{ij}x' + y'(C_{ij}+D_{ij}x') \tag{21}$$

the second term of Equation (12) can be integrated piecewise over the $x'y'$ plane and becomes

$$\iint Jf_{x'x'}\,dx'dy' = -8 \sum_{i=1}^{M-1} \sum_{j=1}^{N-1} H(x-x') \left\{ \frac{J_{2,c}}{k_o} [A_{ij}+B_{ij}x'+y'(C_{ij}+D_{ij}x')] \right.$$

$$\left. + \frac{J_{3,s}}{k_o^2} (B_{ij}+D_{ij}y') - \frac{J_{4,c}}{k_o^2} (C_{ij}+D_{ij}x') - \frac{J_{5,s}}{k_o^3} D_{ij} \right\} \tag{22}$$

where

$$J_{p,c} = \int_1^{\infty} \frac{e^{k_o y' t^2}}{t^p \sqrt{t^2-1}} \cos [k_o(x-x')t]\,dt, \quad p = 2,4 \tag{23}$$

and

$$J_{p,s} = \int_1^{\infty} \frac{e^{k_o y' t^2}}{t^p \sqrt{t^2-1}} \sin [k_o(x-x')t]\,dt, \quad p = 3,5 \tag{24}$$

With $f_{x'}(-L/2,y') = E_j + F_j y'$, the fourth term of Equation (12) can be integrated as

$$\int Jf_{x'}\,dy' = -8 \sum_{j=1}^{N-1} \left[-J_{1,s}(E_j+F_j y') + \frac{F_j}{k_o} J_{3,s} \right] \Bigg|_{x'=-\frac{L}{2}} \tag{25}$$

In Equation (25), the Heaviside function is satisfied by requiring $J_{1,s}$ and $J_{3,s}$ to be zero at $x' = x$.

While $J_{p,c}$ and $J_{p,s}$ include harmonic functions, the numerical evaluation is performed in each cycle of the periodic function

$$k_o(x-x')\ t = \left(n+\frac{1}{2}\right)\pi, \quad n = 0,1,2... \tag{26}$$

When $n = 0$, $t_o = \pi/2k_o(x-x')$ and t_o must be larger than 1. In the region between 1 and t_o, the substitution of variables $u^2 = t^2 - 1$ applied to Equation (23) yields

$$J_{p,c} = \int_0^{\sqrt{t_o^2-1}} \frac{e^{k_o y'(1+u^2)}}{(1+u^2)^{\frac{p+1}{2}}} \cos\left[k_o(x-x')\sqrt{1+u^2}\right] du \tag{27}$$

Equation (27) is more convenient than Equation (23) in numerical computations for $n \leq 1$, but for $n > 1$, Equation (23) is used in the numerical evaluation.

When $k_o y'$ is small, there are many harmonic oscillations before the exponential function decays for large t. In this case the rational-exponential term in Equation (23) is replaced with a simple linear function so that the integral can be done easily. With $a = k_o y'$, $b = k_o(x-x')$, $t_1 = (2n+1/2)\pi$ and $t_2 = (2n+2+1/2)\pi$, $J_{p,c}$ becomes

$$\int_{t_1}^{t_2} \frac{e^{at^2}}{t^p\sqrt{t^2-1}} \cos bt\ dt = \int_{t_1}^{t_2} (B_1 t+B_2) \cos bt\ dt = \frac{B_1}{b}(t_1-t_2) \tag{28}$$

With the same analogy and in this case, $t_1 = 2n\pi$ and $t_2 = (2n+2)\pi$, $J_{p,s}$ is given by

$$\int_{t_1}^{t_2} \frac{e^{at^2}}{t^p\sqrt{t^2-1}} \sin bt\ dt = \int_{t_1}^{t_2} (B_1 t+B_2) \sin bt\ dt = \frac{B_1}{b}(t_1-t_2) \tag{29}$$

In each interval where the integrand becomes zero, B_1 is computed, and with Equations (28) and (29), $J_{p,c}$ and $J_{p,s}$ are approximated, respectively. Values of $J_{p,c}$ and $J_{p,s}$ for a = -0.12 and b = 1.0 are computed and given in Table 2. The first row shows the results of Equation (27) with $t_o = 1.5708$. The second row shows the numerical integral of Equations (23) and (24) with $1.5708 < t < 7.85398$. As shown in Table 2, the integrated results of Equation (27) are dominant in the whole region of computation.

In order to validate the numerical results of Equation (12), two hull forms have been selected: a Wigley hull and an SL7 container ship. The Wigley hull is a mathematical hull form which is represented as

$$f(x,y) = \frac{B}{2}\left(1.0 - \frac{4x^2}{L^2}\right)\left(1.0 - \frac{y^2}{H^2}\right) \tag{30}$$

where L = 20 ft, B = 2 ft, and H = 1.25. The block coefficient of this hull is 0.444. The SL7 is a container ship with a large bulbous bow; its sectional hull offsets are given in Table 3. Its length is 880.5 ft; width, 105.8 ft; and draft, 34.1 ft. The block coefficient of the SL7 is 0.53.

Figure 2 shows the wave profiles of the Wigley hull for $F_n = 0.266$ and 0.452. The wave profiles are computed at the centerplane where z = 0, and the experimental results are measured at the hull surface. For $F_n = 0.266$, the numerical results agree fairly well with the experiment.[5] For $F_n = 0.452$, there is some discrepancy near the bow and the region aft of the midship section. As shown in Reference 1, at higher Froude numbers, the numerical results of various analytical methods do not agree well with the experiment in the bow region. This indicates that the effect of trim and sinkage might be important when the speed is high.

Figure 3 shows the computed wave profiles for the SL7. The agreement between the numerical results and experiment[6] is not satisfactory for this hull. The large bulbous bow might be the cause of the discrepancies. The thin ship theory assumes that hull function is closed at the bow and stern, and the assumption is violated for this hull.

TABLE 2 - NUMERICAL EXAMPLE OF $J_{p,c}$ AND $J_{p,s}$

$k_o y' = -0.12$ AND $k_o(x-x') = 1.0$

Range of Variable u or t	$J_{1,s}$	$J_{2,c}$	$J_{3,s}$	$J_{4,c}$	$J_{5,s}$
0-1.21136 Equation (23)	0.67517	0.27498	0.52425	0.23789	0.42996
1.5708-7.85398 Equation (20)	0.16246	-0.04389	0.04810	-0.00867	0.01476
Total	0.83756	0.23109	0.57235	0.22922	0.44472

TABLE 3 - OFFSET OF SL7 (in feet)

Station	x	y=-34.100 (Keel Line)	-27.280	-20.460	-13.640	-6.820	0.000 (Free Surface)
(FP) 1	-440.250	0.000	7.180	5.366	2.126	0.197	0.200
2	-396.225		8.299	7.148	4.067	2.511	3.350
3	-352.200		9.606	9.087	6.966	6.368	8.400
4	-308.175		10.799	11.505	11.211	12.287	15.200
5	-264.150		12.903	15.653	17.637	20.204	23.100
6	-220.125		17.132	21.555	24.915	28.054	30.950
7	-176.100		23.041	28.056	32.116	35.237	38.050
8	-132.075		29.765	35.474	39.347	41.973	44.100
9	-88.050		36.797	42.158	45.225	47.370	48.800
10	-44.025		42.917	47.737	49.707	51.122	51.750
11	0.000		47.278	51.053	52.298	52.735	52.900
12	44.025		49.033	52.170	52.900	52.900	52.900
13	88.050		48.075	51.406	52.900	52.900	52.900
14	132.075		44.441	49.771	52.233	52.870	52.900
15	176.100		39.333	46.613	49.980	52.246	52.900
16	220.125		31.908	41.359	46.650	50.205	51.750
17	264.150		22.286	33.616	40.036	45.408	48.200
18	308.175		12.867	23.228	31.052	38.069	42.550
19	352.200		5.880	12.958	19.868	27.937	34.250
20	396.225		0.000	3.929	9.303	15.997	23.550
(AP)21	440.250	0.000	0.000	0.000	0.000	3.061	10.600

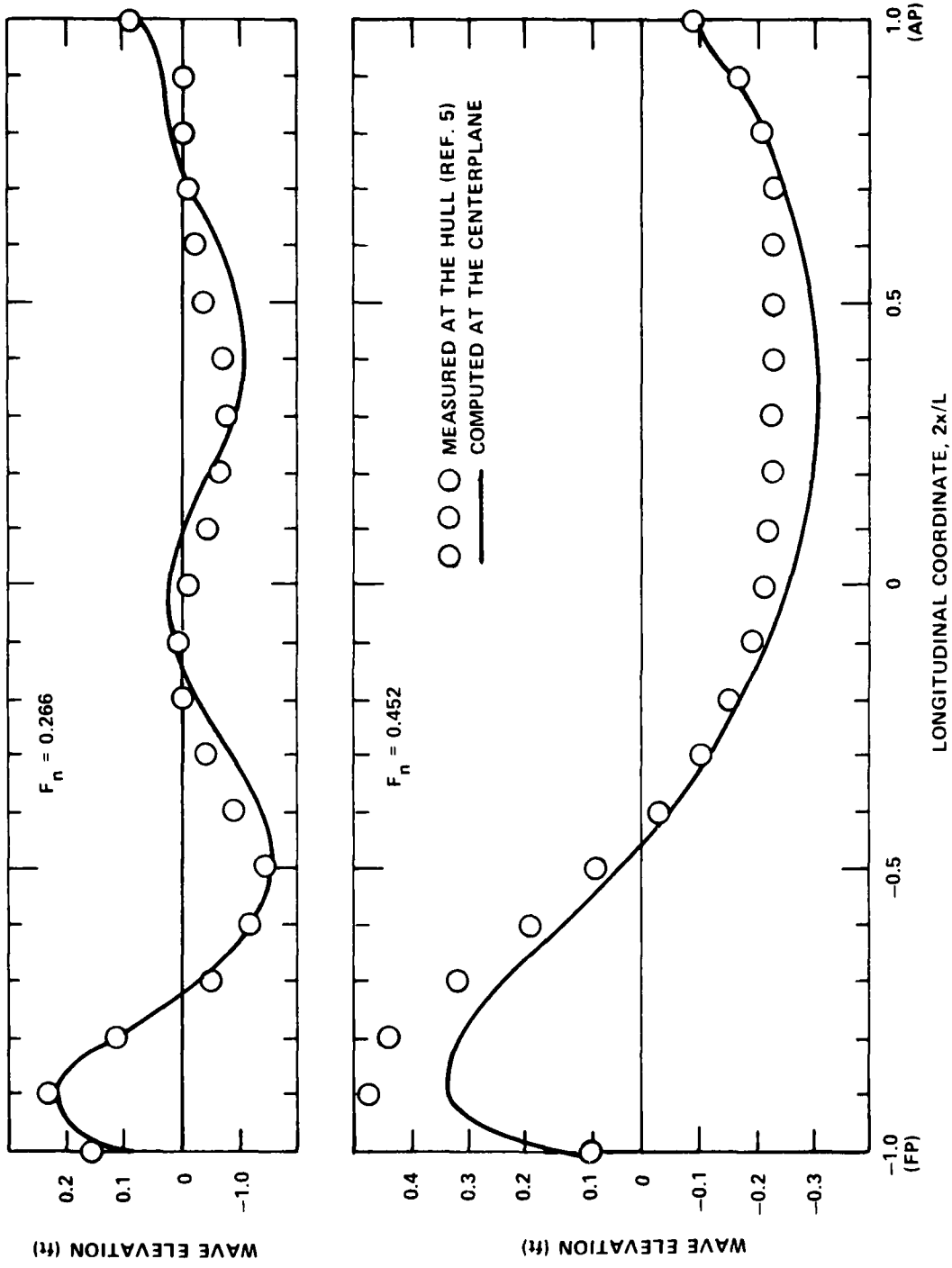

Figure 2 - Wave Profiles of Wigley Hull for F_n = 0.266 and 0.452

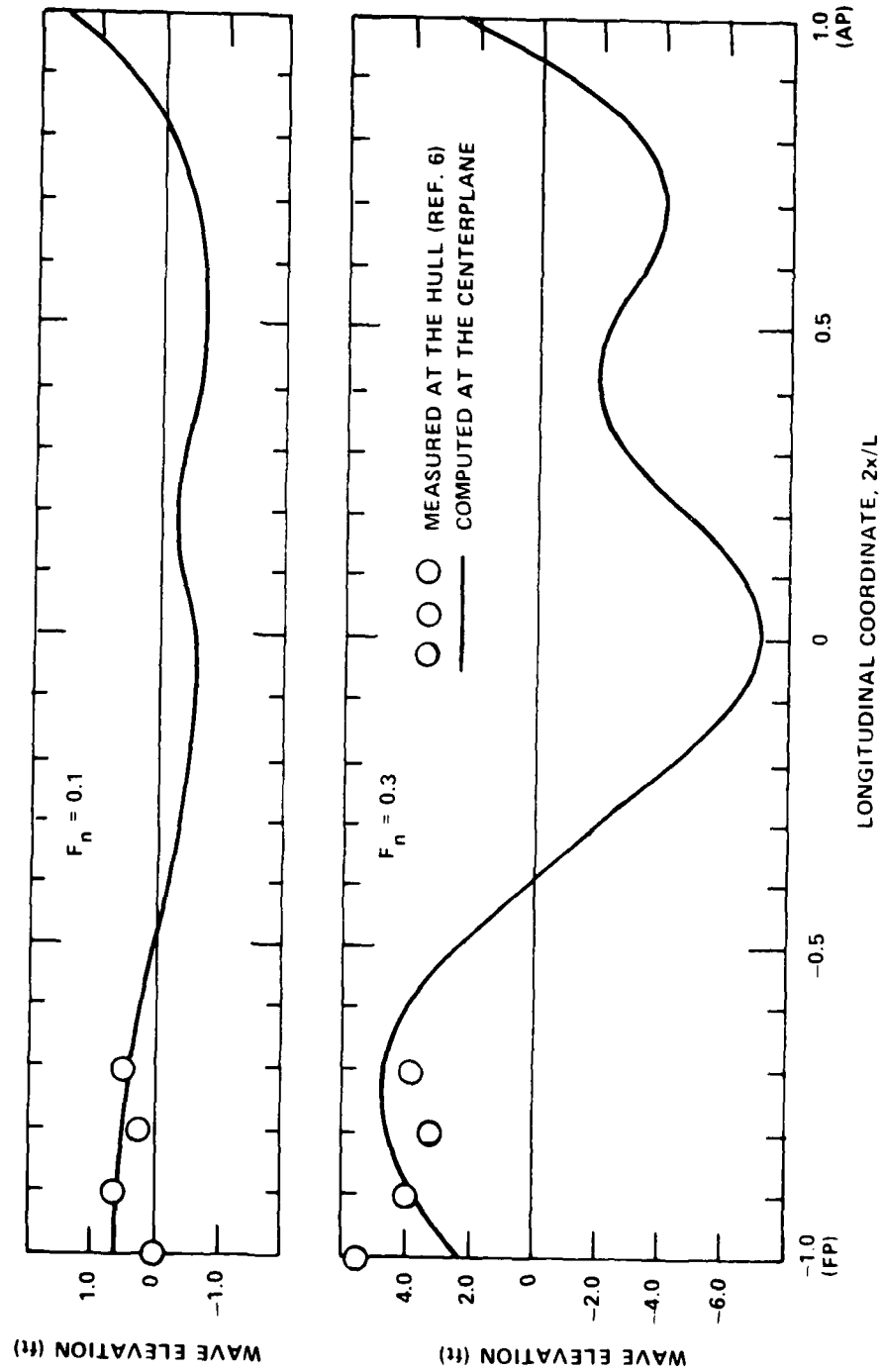

Figure 3 - Wave Profiles of SL7 for F_n = 0.1 and 0.3

CONCLUSIONS

The thin ship theory has been applied for the computation of the free-surface wave height produced by a ship in steady forward motion. For a Wigley hull, the agreement between the computation and experiment is fairly good. However, the numerical results for an SL7 show large discrepancies from the experiment. It seems that the inclusion of the effect of a bulbous bow and transom stern to the present method is necessary. Further, the effects of trim and sinkage should be included in future developments.

ACKNOWLEDGMENT

The author gratefully acknowledges the support of Dr. C.M. Lee.

REFERENCES

1. Bai, K.J. and J.H. McCarthy, Editors of the Proceedings of the Workshop on Ship Wave-Resistance Computations, held at DTNSRDC (Nov 1979).

2. Wehausen, J.V., "Ship Hydrodynamics II - Wave Resistance," Lecture Note NA241, the Department of Naval Architecture and Offshore Engineering, University of California, Berkeley (1972).

3. Hong, Y.S., "Numerical Calculation of Second-Order Wave Resistance," Journal of Ship Research, Vol. 21, No. 2, pp. 94-106 (Jun 1977).

4. Yeung, R.W., "Sinkage and Trim in First-Order Thin-Ship Theory," Journal of Ship Research, Vol. 16, No. 1, pp. 47-59 (Mar 1972).

5. Shearer, J.R. and J.J. Cross, "The Experimental Determination of the Components of Ship Resistance for a Mathematical Model," Transaction of the Royal Institute of Naval Architecture, London, Vol. 107, pp. 459-473 (1965).

6. Lee, C.M. et al., "Prediction of Relative Motion of Ships in Waves," 14th Symposium of Naval Hydrodynamics, University of Michigan (1982).

INITIAL DISTRIBUTION

Copies	
1	CHONR/432/C.M. Lee
2	NRL 1 Code 2027 1 Code 2627
3	USNA 1 Tech Lib 1 Nav Sys Eng Dept 1 Bhattacheryya
2	NAVPGSCOL 1 Library 1 Garrison
1	NADC
1	NELC/Lib
1	NOSC/Lib
1	NCEL/Code 131 Port Hueneme, CA 93043
13	NAVSEA 1 SEA 03R/L. Benen 1 SEA 03R/R. Dilts 1 SEA 03R/N. Kobitz 1 SEA 03R/J. Schuler 1 SEA 05B/P.A. Gale 1 SEA 05R24/J. Sejd 1 SEA 31241/P. Chatterton 1 SEA 321/R.G. Keane, Jr. 1 SEA 3213/E.N. Comstock 1 SEA 3213/W. Livingston 1 SEA 501/G. Kerr 1 SEA 50151/C. Kennel 1 SEA 61433/F. Prout
12	DTIC
1	NSF/Engineering Lib
1	DOT/Lib TAD-491.1
1	NBS/Klebanoff
1	MARAD/Lib
4	U. of Cal/Dept Naval Arch, Berkeley 1 Eng Library 1 Webster 1 Paulling 1 Wehausen
2	U. of Cal, San Diego 1 A.T. Ellis 1 Scripps Inst Lib
2	CIT 1 Aero Lib 1 T.Y. Wu
1	Catholic U. of Amer/ Civil & Mech Eng
1	Colorado State U./Eng Res Cen
1	Florida Atlantic U./Tech Lib
1	U. of Hawaii/St. Denis
1	U. of Illinois/J. Robertson
2	U. of Iowa 1 Library 1 Landweber
1	U. of Kansas/Civil Eng Lib
1	Lehigh U./Fritz Eng Lab Lib
3	MIT 1 Ogilvie 1 Abkowitz 1 Newman

Copies	
2	U. of Mich/NAME 1 Library 1 M. Parsons
1	U. of Notre Dame 1 Eng Lib
2	New York U./Courant Inst 1 A. Peters 1 J. Stoker
4	SIT 1 Breslin 1 Savitsky 1 Dalzell 1 Kim
1	U. of Texas/Arl Lib
2	Southwest Res Inst 1 Applied Mech Rev 1 Abramson
1	Stanford Res Inst/Lib
2	U. of Washington 1 Eng Lib 1 Mech Eng/Adee
3	Webb Inst 1 Library 1 Lewis 1 Ward
1	Woods Hole/Ocean Eng
1	SNAME/Tech Lib
1	Bethlehem Steel/New York/Lib
1	General Dynamics, EB/Boatwright
1	Gibbs & Cox/Tech Info
1	Hydronautics/Library

Copies	
1	Newport News Shipbuilding/Lib
1	Sperry Rand/Tech Lib
1	Sun Shipbuilding/Chief Naval Arch
2	American Bureau of Shipping 1 Lib 1 Cheng
1	Maritime Research Information Service

CENTER DISTRIBUTION

Copies	Code	Name
1	1102	G.D. Elmer
1	1113	G.R. Lamb
1	117	R.M. Stevens
1	1500	W.B. Morgan
1	1504	V.J. Monacella
1	1506	S. Hawkins
1	1520	W.C. Lin
1	1521	W.G. Day
1	1521	A.M. Reed
1	1522	G.F. Dobay
1	1522	M.B. Wilson
1	1522	Y.H. Kim
1	1540	J.H. McCarthy
1	1540	B. Yim
1	1542	Branch Head
1	1560	D. Cieslowski
1	1561	G.C. Cox
1	1561	S.L. Bales
1	1561	W.R. McCreight

Copies	Code	Name
1	1562	D.D. Moran
1	1562	E.E. Zarnick
1	1562	K.K. McCreight
10	1562	Y.S. Hong
1	1563	D.T. Milne
1	1564	J.P. Feldman
1	1564	R.M. Curphey
30	5211.1	Reports Distribution
1	522.1	Unclassified Lib (C)
1	522.2	Unclassified Lib (A)

DTNSRDC ISSUES THREE TYPES OF REPORTS

1. DTNSRDC REPORTS, A FORMAL SERIES, CONTAIN INFORMATION OF PERMANENT TECHNICAL VALUE. THEY CARRY A CONSECUTIVE NUMERICAL IDENTIFICATION REGARDLESS OF THEIR CLASSIFICATION OR THE ORIGINATING DEPARTMENT.

2. DEPARTMENTAL REPORTS, A SEMIFORMAL SERIES, CONTAIN INFORMATION OF A PRELIMINARY, TEMPORARY, OR PROPRIETARY NATURE OR OF LIMITED INTEREST OR SIGNIFICANCE. THEY CARRY A DEPARTMENTAL ALPHANUMERICAL IDENTIFICATION.

3. TECHNICAL MEMORANDA, AN INFORMAL SERIES, CONTAIN TECHNICAL DOCUMENTATION OF LIMITED USE AND INTEREST. THEY ARE PRIMARILY WORKING PAPERS INTENDED FOR INTERNAL USE. THEY CARRY AN IDENTIFYING NUMBER WHICH INDICATES THEIR TYPE AND THE NUMERICAL CODE OF THE ORIGINATING DEPARTMENT. ANY DISTRIBUTION OUTSIDE DTNSRDC MUST BE APPROVED BY THE HEAD OF THE ORIGINATING DEPARTMENT ON A CASE-BY-CASE BASIS.

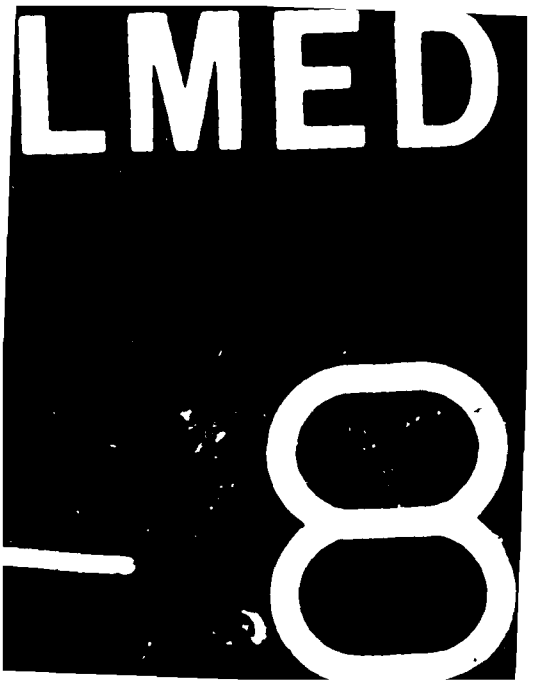
LMED
8